Research Square

Preprints are preliminary reports that have not undergone peer review.
They should not be considered conclusive, used to inform clinical practice,
or referenced by the media as validated information.

Targeting the ROCK2-BACH1-CXCL5 axis alleviates sepsis-induced liver injury by restoring protective neutrophil recruitment

Xu Zhang
Second Affiliated Hospital of Nanchang University
Wen Zeng
Second Affiliated Hospital of Nanchang University
Zuao Wang
Second Affiliated Hospital of Nanchang University
Lai Pengwei
Second Affiliated Hospital of Nanchang University
Haoran Qu
Second Affiliated Hospital of Nanchang University
Jipeng Liu
Second Affiliated Hospital of Nanchang University
Xingchi Zhou
Second Affiliated Hospital of Nanchang University
Jiarong Ye
Second Affiliated Hospital of Nanchang University
Zecheng Jiang
Second Affiliated Hospital of Nanchang University
Chaojie Zhai
Second Affiliated Hospital of Nanchang University
Song Huang
Second Affiliated Hospital of Nanchang University
Xiaohong Du
ndefy02032@ncu.edu.cn

Second Affiliated Hospital of Nanchang University
Leifeng Chen
Second Affiliated Hospital of Nanchang University

Research Article

Keywords: Sepsis-induced liver injury, ROCK2, CXCL5, neutrophil recruitment, BACH1

Posted Date: November 18th, 2026

DOI: https://doi.org/10.21203/rs.3.rs-11545707/v1

License: This work is licensed under a Creative Commons Attribution 4.0 International License.
Read Full License

Additional Declarations: No competing interests reported.

Targeting the ROCK2-BACH1-CXCL5 axis alleviates sepsis-induced liver injury by restoring protective neutrophil recruitment

Xu Zhang[1†], Wen Zeng[1†], Zuao Wang[2, 3, 4], Pengwei Lai[1], Haoran Qu[1], Jipeng Liu[2, 3, 4], Xingchi Zhou[2, 3, 4], Jiarong Ye[2, 3, 4], Zecheng Jiang[2, 3, 4], Chaojie Zhai[2, 3, 4], Song Huang[1], Xiaohong Du[1*], Leifeng Chen[2, 3, 4*]

[1] Department of Anesthesiology, The Second Affiliated Hospital of Nanchang University, Nanchang, Jiangxi Province, 330006, People's Republic of China

[2] Department of Oncology, The Second Affiliated Hospital of Nanchang University, Nanchang, Jiangxi Province, 330006, People's Republic of China

[3] Precision Oncology Medicine Center, Second Affiliated Hospital of Nanchang University, Nanchang, Jiangxi Province, China.

[4] The MOE Basic Research and Innovation Center for the Targeted Therapeutics of Solid Tumors, Nanchang University, Nanchang, China

†These authors contributed equally to this work.

*Correspondence: Leifeng Chen (18770099029@126.com); Xiaohong Du (ndefy02032@ncu.edu.cn).

Competing interests: The authors declare no competing interests.

Abstract

Sepsis-induced liver injury (SILI) is a fatal complication characterized by dysregulated immune responses. While early hepatic recruitment of neutrophils is critical for host defense and bacterial clearance, the molecular brakes that aberrantly restrict this protective mechanism during SILI remain poorly understood. Here, we identify Rho-associated coiled-coil-containing protein kinase 2 (ROCK2) as a pivotal upstream driver of SILI. ROCK2 is markedly upregulated in septic livers, and its genetic deficiency significantly improves survival, attenuates hepatic damage, and suppresses inflammation in septic mice. Furthermore, ROCK2 exacerbates SILI by impairing CXCL5-mediated hepatic neutrophil recruitment. Mechanistically, we uncovered a non-canonical mechanism wherein ROCK2 physically interacts with the transcription factor BACH1, competing with ubiquitin to prevent its proteasomal degradation. This aberrant stabilization enables BACH1 to directly occupy the CXCL5 promoter, silencing its transcription and dampening protective neutrophil infiltration. Overexpression of BACH1 or knockdown of CXCL5 abolished the hepatoprotective effects of ROCK2 deficiency. Moreover, we identified the natural compound epigallocatechin-3-gallate (EGCG) as a potent ROCK2 inhibitor. Pharmacological targeting of ROCK2 with EGCG effectively relieved BACH1-mediated repression, restored CXCL5 expression and neutrophil recruitment, and ameliorated SILI. Collectively, our findings delineate a novel ROCK2-BACH1-CXCL5-neutrophil pathogenic cascade, highlighting a unique kinase-mediated competitive stabilization of a transcription factor, and establish ROCK2 as an actionable therapeutic target for sepsis.

Keywords： Sepsis-induced liver injury；ROCK2；CXCL5；neutrophil recruitment；BACH1

Introduction

Sepsis is a life-threatening organ dysfunction caused by a dysregulated host response to infection, with the liver being one of the earliest affected organs[1, 2]. As a key metabolic and immune organ, the liver is responsible for bacterial clearance and the synthesis of acute-phase proteins and cytokines during sepsis, thereby activating immune defense mechanisms through inflammatory responses[3]. However, excessive inflammation can lead to severe hepatocellular injury, a condition termed sepsis-induced liver injury (SILI)[4]. Epidemiological data indicate an annual incidence of approximately 189 cases per 100,000 adults, with a mortality rate of 26.7%[5]. Notably, mortality surges to 54%–68% in septic patients with concurrent hepatic dysfunction[6]. Despite the severity of this condition, effective targeted therapies remain highly limited, underscoring an urgent need to uncover novel actionable targets and develop efficacious pharmacological interventions for SILI.

During the early phase of sepsis, the rapid mobilization and targeted recruitment of innate immune cells, particularly neutrophils, are fundamental defense mechanisms required for bacterial clearance and tissue homeostasis[7]. This precise spatial navigation is orchestrated by chemokines[8, 9], which exert dual essential functions: directing neutrophils from the vasculature into sites of injury, and activating their antimicrobial and tissue-repair capacities. Dysregulation of this highly coordinated chemokine–neutrophil axis severely compromises host immunity and drives pathological progression in severe inflammatory conditions, including acute respiratory distress syndrome (ARDS), tuberculosis (TB), cystic fibrosis, traumatic brain injury (TBI), sepsis, inflammatory bowel disease (IBD), and multiple cancers[10-17]. Among the key chemotactic factors, CXCL5(C-X-C motif chemokine ligand 5) has emerged as a potent neutrophil chemoattractant[18]. For instance, in experimental peritonitis, robust CXCL5-driven neutrophil infiltration significantly bolsters local bacterial clearance and confers clear survival benefits[19]. However, despite its recognized protective role, the upstream regulatory networks governing CXCL5 transcription and how this protective

chemokine is aberrantly modulated in the specific context of SILI remain completely elusive.

Rho-associated coiled-coil containing protein kinase 2 (ROCK2) is a key effector of the Rho/ROCK signaling pathway and regulates diverse cellular processes including contraction, adhesion, migration, proliferation, and apoptosis[20-22]. In the context of sepsis, ROCK2 has been shown to participate in the pathogenesis of multiple organ injuries, as evidenced by its upregulation in the lungs[23], intestines[24], and kidneys[25], while its knockdown attenuates brain injury and cognitive dysfunction[26]. Notably, ROCK2 overexpression correlates with the progression and poor prognosis of sepsis-associated lung injury[23], underscoring its critical pathogenic role in septic organ damage[27, 28]. Furthermore, within the hepatic microenvironment, ROCK2 is aberrantly upregulated and fuels the progression of metabolic dysfunction-associated steatotic liver disease, liver fibrosis, and hepatocellular carcinoma[29, 30]. Despite its established role in coordinating systemic inflammation and liver pathology, the specific expression profile and functional significance of ROCK2 in SILI remain completely uncharacterized. More importantly, whether ROCK2 serves as the elusive upstream "brake" that paralyzes the protective CXCL5–neutrophil axis during hepatic infection represents a critical, yet unexplored, scientific question.

In the present study, we directly address this critical question by identifying ROCK2 as the definitive upstream repressor of protective immunity in early SILI. We demonstrate that ROCK2 is aberrantly upregulated during early sepsis and actively exacerbates hepatic injury. Mechanistically, we uncover a non-canonical mode of kinase regulation: ROCK2 physically interacts with the transcription factor BACH1, competing with ubiquitin to shield BACH1 from proteasomal degradation. This aberrantly stabilized BACH1 subsequently binds to the CXCL5 promoter, silencing its transcription and thereby blunting the protective recruitment of neutrophils to the liver. Furthermore, we identified the natural compound epigallocatechin-3-gallate (EGCG) as a potent ROCK2 inhibitor capable of dismantling this repressor complex.

Pharmacological targeting with EGCG effectively restored the CXCL5–neutrophil axis and conferred robust protection against SILI. Collectively, our findings not only elucidate a novel kinase-mediated competitive stabilization mechanism but also establish the ROCK2-BACH1-CXCL5-neutrophil axis as a highly actionable therapeutic target for sepsis.

Materials and methods

Animals

All animal experiments were approved by the Ethics Committee for Animal Research at Nanchang University (Approval No. NCULAE-20250331089) and performed in accordance with the Guide for the Care and Use of Laboratory Animals. ROCK2$^{+/-}$ and wild-type (WT) mice (male, 8–16 weeks old) were obtained from GemPharmatech Co., Ltd. (Jiangsu, China) and housed under specific pathogen-free conditions at 22 ± 1°C with a 12 h light/dark cycle.

CLP and LPS

Polymicrobial sepsis was induced by cecal ligation and puncture (CLP) as previously described [31]. Sham-operated mice underwent the same procedure without cecal ligation or puncture. For the LPS-induced sepsis model, mice received a single intraperitoneal injection of LPS (10 mg/kg body weight); sham mice received an equivalent volume of normal saline. All mice were euthanized 48 h post-surgery.

Cell lines and culture

AML12 cells (XBS0422-0209) were obtained from Procell (Wuhan, China); HepG2 cells were kindly provided by HySigen Biosciences Inc. RAW264.7 and THP-1 cells were maintained in our laboratory. All cell lines were authenticated by short tandem repeat (STR) profiling and tested negative for mycoplasma contamination. AML12 cells were cultured in DMEM/F12 (Solarbio, D6501) supplemented with 10% FBS (GIBCO), ITS-G (Procell, PB180429), 1% P/S (Procell, PB180120), and dexamethasone (MCE, 50022). RAW264.7 cells were maintained in DMEM (Solarbio,

12100) with 10% FBS. HepG2 and THP-1 cells were cultured in specialized media (HySigen Biosciences Inc, TCH-G196 and TCH-G361). All cell lines were incubated at 37°C in a humidified atmosphere containing 5% CO_2.

Cell-based sepsis model

To establish an in vitro sepsis model, a co-culture system was employed. RAW264.7 and THP-1 macrophages were stimulated with interferon-gamma (IFN-γ) (50 ng/mL) for 12 h to induce M1 polarization. After confirming that >90% of the cells had transitioned to the M1 phenotype by flow cytometry, the culture supernatant was collected, supplemented with LPS (1 μg/mL), and applied to AML12 or HepG2 cells for 6 h.

Plasmid and shRNA transfection

Lentiviral vectors for ROCK2 knockdown (shROCK2) and overexpression (Flag-ROCK2) were purchased from GeneChem (Shanghai, China). Mouse CXCL5 shRNA- and overexpression-encoding adeno-associated viruses (AAVs), BACH1 overexpression AAV, ROCK2 and BACH1 plasmids, as well as siRNAs targeting BACH1 and CXCL5, were obtained from Hanbio Biotechnology Co., Ltd. The target sequences for all constructs are listed in Table S1.

Reagents and antibodies

CHX were purchased from Selleck, puromycin dihydrochloride and MG-132 were purchased from Sigma. Antibodies and dilution ratios were as follows: anti-ROCK2 (Proteintech, 21645-2-AP; 1:2000) , anti-ROCK2 (Abcam, ab317246; 1:1000), anti-BACH1 (ABclonal, A5393SP; 1:5000), anti-BACH1 (Proteintech, 14018-1-AP; 1:3000),anti-β-actin (Proteintech, 66009-1-Ig; 1:10,000), anti-CXCL5 (Thermo fisher, CXCL5-101AP; 1:1000), anti-p-MYPT1 (Proteintech, 87088-1-RR; 1:2000), anti-MYPT1 (Proteintech, 22117-1-AP; 1:8000), Goat anti-Rabbit IgG (H + L) Cross-Adsorbed Secondary Antibody ((Proteintech, RGAR001; 1:2000), Goat anti-mouse IgG (H + L) cross-adsorbed secondary antibody (Proteintech, RGAM001; 1: 2000).

Western blot

Total protein was extracted from tissues or cells using RIPA lysis buffer. Protein concentrations were determined via the BCA assay, and equal amounts of protein were mixed with loading buffer and denatured at 100°C for 10 min. Samples were resolved by SDS-PAGE (10% or 7.5% gels) and transferred onto 0.22 μm PVDF membranes. The membranes were blocked with 5% non-fat milk for 1 h at room temperature, probed with primary antibodies overnight at 4°C, and then incubated with HRP-conjugated secondary antibodies for 1 h at room temperature. Immunoreactive bands were visualized using an enhanced chemiluminescence (ECL) substrate and quantified with ImageJ software.

RNA extraction and quantitative real-time PCR (qRT-PCR)

Total RNA was extracted from cultured cells or tissues using an RNA extraction kit (R0026, Beyotime) according to the manufacturer's protocol. RNA concentration and purity were measured using a NanoDrop 2000 spectrophotometer (Thermo Fisher Scientific). Reverse transcription was performed using a commercial kit (CW Biotech, Beijing, China). Quantitative real-time PCR (qPCR) was carried out with TB Green® Premix Ex Taq (RR820A, TaKaRa) on a QuantStudio 5 Real-Time PCR System (Applied Biosystems). Gene expression levels were normalized to Gapdh mRNA, and relative quantification was calculated using the $2^{-}\Delta\Delta Cq$ method. All primer sequences are listed in Table S1.

Cell viability

Cell viability was assessed using the CCK-8 assay. Cells were seeded into 96-well plates at a density of 5×10^3 cells per well and cultured for 24 h. After treatment, 10μL of CCK-8 solution (CA1210, Servicebio) was added to each well and incubated for an additional 4 h at 37°C. The absorbance at 450 nm was recorded using a Varioskan LUX multimode microplate reader (Thermo Fisher Scientific).

Enzyme-linked immunosorbent assay (ELISA)

Concentrations of IL-6 (CSB-E04639), TNF-α (CSB-E04741), and IL-1β (CSB-E08054) in cell supernatants or serum samples were measured using commercially available ELISA kits (Solarbio) according to the manufacturer's protocols. The absorbance at 450 nm was recorded using a Varioskan LUX multimode microplate reader (Thermo Fisher Scientific).

Biochemical assay

Serum alanine aminotransferase (ALT) and aspartate aminotransferase (AST) levels were measured using commercially available assay kits (LCSSH-0423W and LCSSH-0424W, AMOY LUNCHANGSHUO BIOTECH, Co., Ltd.) according to the manufacturer's instructions.

Immunohistochemistry (IHC) and immunofluorescence analyses (IF)

Liver tissues were fixed in 4% paraformaldehyde, embedded in paraffin, and sectioned at 4 μm thickness. Sections were deparaffinized with xylene, rehydrated through a graded ethanol series, subjected to antigen retrieval in citrate buffer, and blocked with 5% goat serum for 30 min at room temperature. Subsequently, sections were incubated overnight at 4°C with primary antibodies against ROCK2 (Proteintech, 21645-2-AP; 1:350), BACH1 (Proteintech, 14018-1-AP; 1:800), CXCL5 (Proteintech, 31087-1-AP; 1:200), IL-6 (Servicenio, GB11117; 1:200), IL-1β (Servicenio, GB11113; 1:200), TNFα(Boster, BA013; 1:200), and MPO(Abcam, ab208670; 1:500). For IHC, sections were incubated with an Envision HRP-labeled polymer (DAKO) for 30 min at room temperature, followed by color development with 3,3'-diaminobenzidine (DAB; DAKO) for 10 min. Sections were counterstained with Mayer's hematoxylin for 2 min. For IF, sections were incubated with Alexa Fluor-conjugated secondary antibodies for 30 min at room temperature, and nuclei were counterstained with DAPI for 5 min. Slides were mounted with an anti-fade mounting medium.

Hematoxylin-eosin (HE) staining and histologic examination

Liver tissues were fixed in 4% paraformaldehyde (P1110, Solarbio), embedded in paraffin, and sectioned at 5 μm thickness. Sections were deparaffinized with xylene, rehydrated through a graded ethanol series, stained with hematoxylin and eosin, dehydrated, cleared, and mounted. Histopathological changes were evaluated under an Olympus BH-2 microscope. The severity of liver injury was scored according to a previously described system [32].

Bioinformatics analysis

RNA-seq data (level 3) and corresponding clinical information from 107 sepsis patients were obtained from the GEO data. Gene set enrichment analysis was performed using the GSVA package with the ssGSEA algorithm[33, 34], , and enrichment scores for each pathway were calculated for each sample. The correlation between BACH1 expression and CXCL5-related pathway scores was assessed by Spearman correlation analysis using R software (version 4.0.3).

Co-IP

AML12 and HepG2 cells were lysed in ice-cold RIPA buffer supplemented with PMSF (100:1) for 10 min. Lysates were centrifuged at 12,000 rpm for 5 min, and the supernatants were incubated with 4μg of primary antibody overnight at 4°C with gentle rotation. with the Classic Magnetic Protein A/G IP/Co-IP Kit (Beyotime, P2179S, Shanghai, China) were then added, and the mixture was incubated for an additional 24 h at 4°C with rotation. After centrifugation at 2,500 rpm for 5 min, the beads were collected and washed three times with ice-cold RIPA buffer. Bound proteins were eluted by boiling in 60 μL of 1× SDS sample buffer for 2 min and subjected to western blotting or liquid chromatography-tandem mass spectrometry (LC-MS/MS).

LC-MS/MS analysis

For LC-MS/MS analysis, protein samples were prepared by immunoprecipitation with anti-ROCK2 antibody as described above. The immunoprecipitated complexes were resolved by SDS-PAGE, and the gels were stained with Coomassie Brilliant Blue for 3

h, followed by overnight destaining. Protein bands of interest were excised and subjected to in-gel tryptic digestion, followed by LC-MS/MS analysis as previously described [35].

Chromatin immunoprecipitation (ChIP) assay

ChIP assays were performed as previously described [36]. Briefly, samples (2–4 g) were washed twice with ice-cold PBS, cross-linked with 1% formaldehyde for 10 min at room temperature, and quenched with glycine (final concentration 125 mM). After lysis on ice, chromatin was sonicated to an average fragment size of 200–500 bp. A 20 μL aliquot of sheared chromatin was saved as input DNA, and 100 μL was incubated overnight at 4°C with 10 μg of anti-BACH1 antibody (A22230; ABclonal) or normal rabbit IgG (2729S, CST). Protein A/G agarose beads (30 μL) were then added and incubated for an additional 3 h. The beads were sequentially washed once with buffer A (20 mM Tris-HCl pH 8.1, 50 mM NaCl, 2 mM EDTA, 1% Triton X-100, 0.1% SDS), twice with buffer B (10 mM Tris-HCl pH 8.1, 250 mM LiCl, 1 mM EDTA, 1% NP-40, 1% sodium deoxycholate), and twice with TE buffer (10 mM Tris-HCl pH 7.5, 1 mM EDTA). Immune complexes were eluted with 300 μL of elution buffer (100 mM $NaHCO_3$, 1% SDS), treated with RNase A (8 μg/mL) at 65°C for 6 h, followed by proteinase K (345 μg/mL) at 45°C overnight. Purified DNA was analyzed by qPCR using the primers listed in Table S1. Reactions were performed with ChamQ SYBR Color qPCR Master Mix, and enrichment was calculated using the $2^{-}\Delta\Delta Cq$ method [37] after normalization to the input.

Dual luciferase reporter assay

To construct the firefly luciferase reporter plasmid pGL3-CXCL5pro, the 2000-bp promoter region upstream of the mouse *Cxcl5* transcription start site was amplified and cloned into the pGL3-Basic vector via NheI and XhoI sites, upstream of the luciferase coding sequence. The overexpression plasmids pcDNA3.1-BACH1 and pcDNA3.1-Mafk were generated by inserting the full-length coding sequences (CDS) of mouse Bach1 and Mafk, respectively, into the pcDNA3.1(+) vector using BamHI

and XhoI sites. All constructs were verified by DNA sequencing. For the dual-luciferase reporter assay, HEK293T cells were seeded in 24-well plates at 1×10^5 cells per well and cultured overnight. Cells were co-transfected with 400 ng of firefly luciferase reporter (pGL3-Basic or pGL3-CXCL5pro), 400 ng of overexpression plasmid (empty pcDNA3.1, pcDNA3.1-BACH1, or pcDNA3.1-MAFK), and 50 ng of pRL-TK (internal control) per well using Lipofectamine™ 2000 (Invitrogen). At 48 h post-transfection, cells were lysed, and firefly and Renilla luciferase activities were sequentially measured with the Dual-Luciferase® Reporter Assay System (Promega). Firefly activity was normalized to Renilla activity, and each transfection was performed in triplicate. The target sequences for all constructs are listed in Table S1.

Statistical analysis

GraphPad Prism (GraphPad Inc.) software (version 26.0, IBM, USA) was used for statistical analysis. Student's t-test was used to compare two groups,while one-way ANOVA was employed for comparisons involving more than two groups. Data were presented as mean ± standard deviation (SD),and $p < 0.05$ was considered statistically significant.

DATA AVAILABILITY

The data supporting the findings of this study are available from the corresponding author upon reasonable request

Results

1. ROCK2 is upregulated in early sepsis-associated liver injury

To investigate the expression and potential role of ROCK2 in sepsis-associated liver injury, we first established an in vitro hepatocyte injury model. Macrophages were stimulated with IFN-γ to induce M1 polarisation (Fig. S1A), and the resulting conditioned medium (M1-CM) was collected and combined with LPS to treat hepatocytes (M1-CM + LPS), thereby recapitulating the inflammatory

297 microenvironment of sepsis (Fig. 1A). CCK-8 assays showed that M1-CM + LPS
298 markedly impaired hepatocyte viability (Fig. 1B). Transcriptomic sequencing identified
299 ROCK2 as one of the most significantly upregulated genes (Fig. 1C), and KEGG
300 enrichment analysis revealed enrichment of inflammation-related signalling pathways
301 (Fig. 1D). Western blotting and ELISA further confirmed that ROCK2 protein
302 expression and the levels of IL-6, IL-1β, and TNF-α were significantly increased
303 following M1-CM + LPS treatment (Fig. 1E).

304 Subsequently, to assess the *in vivo* relevance of these findings, we established
305 mouse models of sepsis using either caecal ligation and puncture (CLP) or LPS
306 challenge. The CLP model more closely recapitulates the polymicrobial infection and
307 progressive pathophysiological changes observed in clinical sepsis (Fig. 1F). Survival,
308 the murine sepsis score (MMS), and serum alanine aminotransferase (ALT) and
309 aspartate aminotransferase (AST) levels were assessed at the indicated time points. In
310 both models, septic mice exhibited reduced survival, higher MMS values, and elevated
311 serum ALT and AST levels (Fig. 1G–I). H&E staining revealed hepatocellular necrosis,
312 vacuolar degeneration, and inflammatory cell infiltration (Fig. 1K). Western blotting
313 showed that hepatic ROCK2 expression was increased in both CLP- and LPS-
314 challenged mice (Fig. 1J), and immunofluorescence analysis further showed
315 concomitant increases in ROCK2 and inflammatory cytokine expression (Fig. 1L, M).
316 Collectively, these findings demonstrated that ROCK2 is markedly upregulated during
317 early sepsis-associated liver injury and is closely associated with the inflammatory
318 response.

319 **2. ROCK2 deficiency ameliorates sepsis-associated liver injury**

320 To determine the functional significance of ROCK2, we established stable
321 ROCK2-knockdown AML12 and HepG2 cell lines (Fig. 2A). The cells were exposed
322 to M1-CM + LPS to mimic the inflammatory microenvironment. Western blotting
323 confirmed efficient ROCK2 knockdown (Fig. 2B), whereas ELISA showed that
324 ROCK2 knockdown significantly reduced the secretion of IL-6, IL-1β, and TNF-α (Fig.

2C). For the *in vivo* experiments, we generated ROCK2 heterozygous knockout (ROCK2+/−) mice, as homozygous deletion was lethal (Fig. 2D). Compared with wild-type mice subjected to CLP, ROCK2+/− mice showed significantly improved survival (Fig. 2E), lower MMS values (Fig. 2F), and reduced serum ALT and AST levels (Fig. 2G). H&E staining revealed markedly attenuated liver injury in ROCK2+/− mice (Fig. 2H). Western blotting (Fig. 2I), immunohistochemistry, and immunofluorescence analyses (Fig. 2J–L) further confirmed that ROCK2 and inflammatory cytokine expression were significantly reduced in the livers of ROCK2+/− mice. These findings comfirmed that ROCK2 deficiency markedly ameliorates sepsis-associated liver injury.

3. ROCK2 deficiency promotes CXCL5-mediated neutrophil recruitment and ameliorates sepsis-associated liver injury

Although ROCK2 deficiency alleviated liver injury, the downstream effector responsible for this protection remained unclear. CXCL5 is a key neutrophil chemoattractant and has been reported to exert protective effects during early sepsis. We therefore investigated whether ROCK2 regulates sepsis-associated liver injury through CXCL5. Transcriptomic sequencing of M1-CM + LPS-treated AML12 cells with stable ROCK2 knockdown identified CXCL5 as one of the most significantly upregulated chemokines (Fig. 3A). KEGG enrichment analysis highlighted chemokine-related signalling pathways following ROCK2 knockdown (Fig. 3B). To validate this finding, ROCK2 was either overexpressed or knocked down in AML12 and HepG2 cells. Western blotting and qPCR demonstrated an inverse regulatory relationship between ROCK2 and CXCL5 (Fig. 3C, D).

To define the functional role of CXCL5 downstream of ROCK2, we established a liver-specific CXCL5-overexpression mouse model by tail-vein injection of a CXCL5-overexpressing adenovirus (Ad-OeCXCL5; Fig. 3E). Successful hepatic overexpression of CXCL5 was confirmed by western blotting and qPCR (Fig. 3F). Compared with control mice, Ad-OeCXCL5 mice exhibited improved survival, lower MMS values, and reduced serum ALT and AST levels after CLP (Fig. 3G–I).

Immunofluorescence analysis further showed increased CXCL5 expression, reduced IL-6, IL-1β, and TNF-α expression, and markedly enhanced infiltration of MPO-positive neutrophils (Fig. 3J, K). To further examine the endogenous regulation of CXCL5 by ROCK2 deficiency, we performed complementary experiments in ROCK2+/− mice. Western blotting showed that CXCL5 protein expression was significantly higher in the CLP + ROCK2+/− group than in the CLP group; consistent results were obtained in the LPS model (Fig. 3L). Immunohistochemical staining further confirmed these findings (Fig. 3M). Thus, CXCL5 overexpression was sufficient to recapitulate the hepatoprotective effect and neutrophil recruitment induced by ROCK2 deficiency.

4. CXCL5 is a critical downstream effector of ROCK2

To determine whether CXCL5 is required for the protective effect of ROCK2 knockdown, CXCL5 was simultaneously silenced in ROCK2-knockdown cells. Western blotting showed that siCXCL5 reversed the shROCK2-induced increase in CXCL5 expression (Fig. 4A), while ELISA revealed a corresponding reversal in inflammatory cytokine secretion (Fig. 4B).

For the in vivo experiments, a CXCL5-knockdown adenovirus (Ad-shCXCL5) was administered to ROCK2+/− mice by tail-vein injection to establish a model with concomitant ROCK2 and CXCL5 deficiency (Fig. 4C). Compared with the CLP + ROCK2+/− group, mice in the CLP + Ad-shCXCL5 + ROCK2+/− group showed reduced survival, higher MMS values, and elevated serum ALT and AST levels (Fig. 4D–F). H&E staining, immunohistochemistry, and immunofluorescence analyses revealed aggravated liver injury, restored inflammatory cytokine expression, and reduced neutrophil infiltration (Fig. 4G, I–K). Western blotting confirmed that the increase in CXCL5 expression was reversed (Fig. 4H). These findings demonstrate that CXCL5 silencing abolishes the protective effect mediated by ROCK2 deficiency, establishing CXCL5 as an essential downstream effector of ROCK2.

5. BACH1 is a transcriptional repressor of CXCL5

To delineate the molecular mechanism by which ROCK2 regulates CXCL5, we performed co-immunoprecipitation coupled with mass spectrometry (Co-IP-MS) in M1-CM + LPS-stimulated AML12 cells and identified BACH1 as a candidate ROCK2-binding protein (Fig. 5A, B). Endogenous Co-IP assays in AML12 and HepG2 cells further validated the interaction between ROCK2 and BACH1 (Fig. 5C).

Previous studies have identified BACH1 as a transcriptional repressor in several inflammatory diseases[38, 39], leading us to hypothesise that it may mediate the transcriptional regulation of CXCL5 downstream of ROCK2. Analysis of a Gene Expression Omnibus dataset revealed a significant inverse correlation between BACH1 and CXCL5 expression ($p = 0.017$; Fig. 5D). Western blotting and qPCR showed that BACH1 knockdown increased CXCL5 expression (Fig. 5E). To determine whether BACH1 directly represses CXCL5 transcription, we performed dual-luciferase reporter and chromatin immunoprecipitation-qPCR (ChIP-qPCR) assays. Because BACH1 frequently heterodimerises with MAFK to enhance its transcriptional regulatory activity, we constructed a pGL3-CXCL5pro plasmid containing the CXCL5 promoter and expression plasmids for BACH1 and MAFK (Fig. 5F). Dual-luciferase reporter assays showed that BACH1 significantly suppressed CXCL5 promoter activity, with stronger repression observed when BACH1 and MAFK were co-expressed (Fig. 5G). For ChIP-qPCR, DNA fragments bound by BACH1 were enriched using a BACH1-specific antibody, and three primer pairs targeting the CXCL5 promoter (Primer 1, Primer 2, and Primer 3) were used for qPCR analysis. BACH1 bound to the P1, P2, and P3 regions of the CXCL5 promoter (Fig. 5H). Together, these findings establish BACH1 as a direct transcriptional repressor of CXCL5.

6. BACH1 mediates ROCK2-dependent regulation of CXCL5

To determine whether BACH1 acts downstream of ROCK2 to regulate CXCL5, BACH1 was overexpressed in ROCK2-knockdown cells. Western blotting showed that BACH1 overexpression reversed the shROCK2-induced increase in CXCL5 expression, and ELISA revealed a corresponding restoration of inflammatory cytokine secretion

(Fig. 6A, B). For the *in vivo* experiments, a BACH1-overexpressing adenovirus (Ad-OeBACH1) was administered to ROCK2+/− mice by tail-vein injection to generate a liver-specific model combining reduced ROCK2 expression with BACH1 overexpression (Fig. 6C). Compared with the CLP + ROCK2+/− group, mice in the CLP + Ad-OeBACH1 + ROCK2+/− group showed reduced survival, higher MMS values, and elevated serum ALT and AST levels (Fig. 6D–F). Serum ALT and AST levels were also increased in the LPS model (Fig. 6G). H&E staining, immunohistochemistry, and immunofluorescence analyses revealed aggravated liver injury, restored inflammatory cytokine expression, and reduced neutrophil infiltration (Fig. 6H–K). Western blotting confirmed that the increase in CXCL5 expression was reversed (Fig. 6L). Collectively, these findings identify BACH1 as the critical molecular link between ROCK2 and CXCL5.

7. ROCK2 inhibits BACH1 ubiquitination and degradation by competing with ubiquitin

Our preceding western blotting results showed that ROCK2 overexpression increased BACH1 protein abundance, whereas ROCK2 knockdown decreased it; however, BACH1 mRNA levels remained unchanged (Fig. S7A), suggesting post-translational regulation. BACH1 is known to be degraded through the ubiquitin-proteasome pathway. Co-IP confirmed the association of BACH1 with ubiquitin (Fig. 7A), and MG132 treatment induced time-dependent accumulation of BACH1 protein (Fig. 7B). In the presence of MG132, altering ROCK2 expression no longer affected BACH1 abundance (Fig. 7C), indicating that ROCK2 regulates BACH1 degradation. AML12 and HepG2 cells co-transfected with Flag-BACH1 and HA-ROCK2 were subsequently treated with cycloheximide (CHX) to block de novo protein synthesis. Western blotting showed that ectopic ROCK2 expression significantly prolonged the half-life of exogenous BACH1 (Fig. 7D, E), further supporting that ROCK2 stabilises BACH1 by inhibiting its degradation.

Our previous work and published studies have shown that ubiquitin-like proteins, such as FAT10, can inhibit ubiquitin-mediated substrate degradation by competing with ubiquitin for substrate binding[40] . We therefore investigated whether ROCK2 regulates BACH1 through a similar mechanism. Co-IP showed that ROCK2 knockdown enhanced BACH1 ubiquitination, whereas ROCK2 overexpression reduced it (Fig. 7F). To determine whether ROCK2 and ubiquitin compete for BACH1 binding, we performed dose-gradient Co-IP assays. Increasing levels of ectopic ROCK2 progressively enhanced the formation of ROCK2-BACH1 complexes while reducing the formation of ubiquitin-BACH1 complexes (Fig. 7G, H). These findings indicate that ROCK2 competes with ubiquitin for BACH1 binding, thereby suppressing ubiquitin-proteasome-dependent degradation and stabilising the BACH1 protein.

8. The natural product EGCG ameliorates sepsis-associated liver injury by targeting ROCK2

To explore the translational potential of this signalling axis, we screened a natural-product small-molecule library and performed molecular docking, identifying epigallocatechin-3-gallate (EGCG) as a candidate compound (Fig. 8A). We first assessed the cytotoxicity of EGCG in hepatocytes. CCK-8 assays showed that treatment with 0–50 μM EGCG for 12 h did not reduce cell viability (Fig. 8B). To evaluate the inhibitory effect of EGCG on ROCK2 activity, we measured the phosphorylation of MYPT1, a downstream substrate of ROCK2. EGCG reduced the p-MYPT1/MYPT1 ratio in a concentration-dependent manner over the range of 0–50 μM, with the strongest inhibition observed at 50 μM (Fig. 8C). Because 50 μM produced the greatest inhibitory effect while maintaining cell viability, this concentration was used in subsequent experiments. In ROCK2-overexpressing AML12 and HepG2 cells, treatment with 50 μM EGCG reduced ROCK2 and BACH1 expression and restored CXCL5 expression (Fig. 8D). In the M1-CM + LPS-induced inflammatory model, EGCG suppressed the ROCK2-BACH1 axis, upregulated CXCL5, and reduced the secretion of IL-6, IL-1β, and TNF-α (Fig. 8E, F).

To further evaluate the *in vivo* efficacy of EGCG, mice received intraperitoneal EGCG (8 mg/kg) beginning 24 h after CLP, followed by a second dose at 48 h. Compared with the CLP group, EGCG-treated mice showed improved survival, lower MMS values, and reduced serum ALT and AST levels (Fig. 8G–I). EGCG also reduced serum ALT and AST levels in the LPS model (Fig. 8J). H&E staining revealed attenuated liver injury (Fig. 8K). Western blotting (Fig. 8L) and immunohistochemistry (Fig. 8M) showed that EGCG reduced ROCK2 and BACH1 expression, increased CXCL5 expression, decreased inflammatory cytokine expression, and enhanced MPO-positive neutrophil infiltration. Collectively, EGCG inhibited ROCK2 activity both in vitro and in vivo, increased CXCL5 expression, promoted neutrophil recruitment, and alleviated sepsis-associated liver injury, supporting ROCK2 as a therapeutic target with translational potential.

Discussion

Sepsis is a life-threatening organ dysfunction caused by a dysregulated host response to infection[41], with the liver being one of the earliest affected organs[42]. Despite advances in understanding the pathological mechanisms of sepsis-induced liver injury (SILI), effective targeted therapeutic strategies remain largely elusive[43]. The present study provides compelling evidence that ROCK2 serves as a central pathogenic kinase driving immunoparalysis and inflammation in early SILI. Here, we delineate a non-canonical mechanism wherein ROCK2 competes with ubiquitin for BACH1 binding, thereby shielding BACH1 from proteasomal degradation. This aberrantly stabilized BACH1 directly represses CXCL5 transcription, blunting essential neutrophil recruitment to the infected liver. Targeting this axis with the natural compound EGCG effectively restored immune defense and alleviated SILI, offering a promising therapeutic avenue for this devastating disease (Fig. 8N).

As a key downstream effector of Rho GTPases, ROCK2 is conventionally recognized for its role in regulating cytoskeletal dynamics, such as cell migration and contraction[44]. Recently, emerging evidence has implicated ROCK2 in the pathogenesis

of sepsis and systemic inflammation. In sepsis-associated injury, Liu et al. demonstrated[45] that ROCK2 exacerbates pulmonary inflammation and pathological damage via NF-κB signaling activation. Similarly, Zhu et al. reported[46] that ROCK2 promotes neuronal apoptosis and glial injury in CLP-challenged rats, effects that were mitigated by the ROCK inhibitor Fasudil. In the context of liver disease, a recent study published[47] in Cell revealed that ROCK2 drives liver fibrosis progression through a vasocrine axis involving endothelial fenestration loss, paracrine profibrotic factor secretion, hepatic stellate cell activation, and subsequent collagen deposition. Despite its established deleterious roles in systemic inflammation and chronic liver diseases, its functional significance in acute SILI remained completely unknown. To the best of our knowledge, this is the first study to investigate the involvement of ROCK2 in SILI. Here, we confirmed that ROCK2 is highly expressed in both liver tissues and cells under SILI conditions. *In vitro* and *in vivo* experiments demonstrated that ROCK2 knockdown improves survival, reduces serum AST/ALT levels, and alleviates hepatic histopathological damage in SILI mice. Collectively, these findings suggest that ROCK2 may serve as a potential biomarker and therapeutic target for SILI.

During the early phase of sepsis, the rapid mobilization and targeted recruitment of innate immune cells, particularly neutrophils, serve as indispensable defense mechanisms for bacterial clearance and hepatic tissue homeostasis[48]. While CXCL5 has been widely recognized as a potent neutrophil chemoattractant[49], conferring clear survival benefits and robust bacterial clearance in severe inflammatory conditions such as experimental peritonitis[19], the upstream regulatory networks governing its aberrant modulation in SILI have remained completely elusive. Our study successfully bridges this critical knowledge gap by identifying ROCK2 as the definitive upstream repressor of the CXCL5-neutrophil axis. We demonstrated that in the highly inflammatory microenvironment of the septic liver, aberrantly upregulated ROCK2 acts as a pathological “immunological brake” that paralyzes protective innate immunity. By suppressing CXCL5 expression, ROCK2 effectively blinds the precise spatial

navigation of neutrophils, preventing their crucial influx from the vasculature into the sites of hepatic injury. Strikingly, targeted ablation of ROCK2 or direct hepatic overexpression of CXCL5 fully restored this vital chemotactic gradient, driving robust neutrophil infiltration, suppressing excessive inflammatory cytokine storms, and markedly ameliorating liver necrosis. These findings not only validate the indispensable protective role of CXCL5-mediated early immune responses but also firmly establish ROCK2 as the elusive "master switch" that orchestrates the dysregulation of this crucial chemokine network during SILI.

Next, we further investigated the mechanism by which ROCK2 regulates the CXCL5 expression. BACH1, which forms heterodimers with small Maf proteins to bind Maf recognition elements in target gene promoters, functions as a transcriptional repressor[38]. Recent studies have highlighted its crucial role in sepsis-related inflammation: BACH1 exacerbates oxidative damage to promote sepsis-associated acute lung injury[50], while BACH1 knockout significantly improves survival and attenuates hepatic and systemic inflammation in CLP-challenged mice[51]. Nevertheless, whether BACH1 directly represses CXCL5 transcription to limit neutrophil recruitment in SILI remains unknown. Our findings revealed that the protein expression of BACH1 was remarkably reduced after ROCK2 knockdown. Meanwhile, BACH1 directly binds to the CXCL5 promoter and BACH1 significantly suppressed CXCL5 promoter activity, with stronger repression observed when BACH1 and MAFK were co-expressed. BACH1 overexpression reversed the shROCK2-induced increase in CXCL5 expression, and ELISA revealed a corresponding restoration of inflammatory cytokine secretion. Moreover, *in vivo* experiments confirmed that forced BACH1 expression in ROCK2$^{+/-}$ mice reversed the rescue of CXCL5 production and neutrophil infiltration, firmly establishing BACH1 as the critical link between ROCK2 and CXCL5. Collectively, we demonstrated that ROCK2 exacerbates sepsis-induced liver injury by repressing CXCL5 production through a BACH1-dependent mechanism.

We further investigated the mechanism by which ROCK2 regulates BACH1. Our previous studies demonstrated that ROCK2 promotes hepatocellular carcinoma cell proliferation by inhibiting CDC25A ubiquitination and degradation[52], enhances invasion and metastasis of hepatocellular carcinoma cells by modulating MMP2 ubiquitination[53], and facilitates osteosarcoma growth and metastasis by regulating PFKFB3 ubiquitination [54]. These findings collectively indicate that ROCK2 stabilizes its substrates by suppressing their ubiquitin-proteasome degradation; however, the precise molecular details remain to be elucidated. In the present study, we found that ROCK2 stabilizes BACH1 expression by affecting its ubiquitination levels. Mechanistically, we confirmed that ROCK2 directly interacts with BACH1 in hepatocytes, and that BACH1 is degraded via the ubiquitin-proteasome pathway. Treatment with the proteasome inhibitor MG132 abolished the effect of ROCK2 modulation on BACH1 protein levels, whereas cycloheximide (CHX) chase assays revealed that ROCK2 overexpression prolonged the half-life of BACH1, indicating that ROCK2 is involved in proteasome-mediated degradation of BACH1. Furthermore, increasing exogenous ROCK2 led to elevated levels of the ROCK2–BACH1 complex and concomitantly reduced levels of the Ub–BACH1 complex, demonstrating that ROCK2 competes with ubiquitin for binding to BACH1, thereby stabilizing BACH1 protein. Collectively, these results suggest that ROCK2 promotes SILI by potentiating BACH1-mediated transcriptional repression of CXCL5, and that targeting the ROCK2/BACH1 axis may represent a potential therapeutic strategy for SILI.

While our genetic models firmly establish ROCK2 as a driving force in SILI, translating these findings into clinical practice necessitates safe and effective pharmacological interventions. Although classical ROCK inhibitors (such as Fasudil) have shown experimental efficacy in inflammatory models[55], their clinical systemic application is often hindered by dose-limiting cardiovascular side effects, particularly hypotension[56]. Therefore, discovering safer alternatives, especially from structurally diverse natural compounds, is of great clinical significance. To explore the translational

potential of this signaling axis, we performed screening of a natural product library combined with molecular docking and identified epigallocatechin gallate (EGCG) as a candidate ROCK2 inhibitor. While EGCG is widely renowned for its broad anti-inflammatory properties[57], its precise direct kinase targets in sepsis have remained largely ambiguous. Here, we demonstrate for the first time that EGCG confers potent protective effects specifically by targeting ROCK2. The suppression of ROCK2 activity by EGCG was confirmed by decreased p-MYPT1/MYPT1 ratios, and the reversal of BACH1 upregulation and CXCL5 downregulation in ROCK2-overexpressing cells further verified that the effects of EGCG are indeed mediated through the ROCK2-BACH1 axis. Crucially, in vivo, a therapeutic regimen starting at 24 h post-CLP markedly improved survival, reduced transaminase levels, and attenuated liver injury. This delayed treatment paradigm, which mirrors the realistic clinical setting of late-stage intervention, substantially strengthens the translational relevance of our findings and highlights EGCG as a promising therapeutic agent for SILI.

In conclusion, our study uncovers a previously unrecognized pathogenic mechanism in early SILI driven by the ROCK2-BACH1-CXCL5 regulatory axis. Pathologically, ROCK2 acts as an aberrant immunological brake by competitively stabilizing the repressor BACH1, which subsequently blunts CXCL5-mediated neutrophil recruitment and paralyzes early innate defense. Importantly, targeted intervention of this axis, either through genetic ablation or the natural compound EGCG, successfully reverses this immunoparalysis and restores hepatic tissue homeostasis. Beyond unveiling a novel mechanism of kinase-mediated transcription factor stabilization, this work establishes a sequential signaling cascade linking kinase activity to innate immunity. Ultimately, targeting the ROCK2 pathway offers a compelling therapeutic strategy to combat systemic inflammation and sepsis-induced organ dysfunction.

Declarations

Ethics approval and consent to participate

All animal experiments were approved by the Ethics Committee for Animal Research at Nanchang University (Approval No. NCULAE-20250331089) and performed in accordance with the approved protocol and relevant guidelines and regulations. This study did not involve human participants, human data, or human tissue.

Consent for publication

Not applicable.

Availability of data and materials

The data supporting the findings of this study are available from the corresponding author upon reasonable request.

Competing interests

The authors declare no competing interests.

Funding

This work was supported by grants from the National Natural Science Foundation of China (82160364) and the Project of the Jiangxi Provincial Department of Science and Technology (20232BCJ22016).

Authors' contributions

Xiaohong Du and Leifeng Chen were responsible for supervising the project, providing funding support, and revising the first draft. Xu Zhang and Wen Zeng carried out major western blotting, bioinformatics, cellular and animal studies, and wrote the original draft. Zu'ao Wang carried out western blotting and cellular and animal studies. Pengwei Lai was responsible for immunohistochemistry. Haoran Qu performed some in vivo animal experiments. Jipeng Liu, Xingchi Zhou, and Zecheng Jiang conducted immunofluorescence staining assays. Jiarong Ye performed enzyme-linked immunosorbent assays. Song Huang and Chaojie Zhai conducted flow cytometry assays. All authors read and approved the final manuscript.

Acknowledgements

Not applicable.

References

1. Singer M, Deutschman CS, Seymour CW, et al. The Third International Consensus Definitions for Sepsis and Septic Shock (Sepsis-3). *JAMA*. Feb 23 2016;315(8):801-10. doi:10.1001/jama.2016.0287
2. Guo Y, Guo W, Chen H, Sun J, Yin Y. Mechanisms of sepsis-induced acute liver injury: a comprehensive review. *Front Cell Infect Microbiol*. 2025;15:1504223. doi:10.3389/fcimb.2025.1504223
3. Sun J, Zhang J, Wang X, et al. Gut-liver crosstalk in sepsis-induced liver injury. *Crit Care*. Oct 19 2020;24(1):614. doi:10.1186/s13054-020-03327-1
4. Strnad P, Tacke F, Koch A, Trautwein C. Liver - guardian, modifier and target of sepsis. *Nat Rev Gastroenterol Hepatol*. Jan 2017;14(1):55-66. doi:10.1038/nrgastro.2016.168
5. Rudd KE, Johnson SC, Agesa KM, et al. Global, regional, and national sepsis incidence and mortality, 1990-2017: analysis for the Global Burden of Disease Study. *Lancet*. Jan 18 2020;395(10219):200-211. doi:10.1016/S0140-6736(19)32989-7
6. Yan J, Li S, Li S. The role of the liver in sepsis. *Int Rev Immunol*. Nov-Dec 2014;33(6):498-510. doi:10.3109/08830185.2014.889129
7. Zhang J, Shao Y, Wu J, et al. Dysregulation of neutrophil in sepsis: recent insights and advances. *Cell Commun Signal*. Feb 14 2025;23(1):87. doi:10.1186/s12964-025-02098-y

8. Kobayashi Y. The role of chemokines in neutrophil biology. *Front Biosci*. Jan 1 2008;13:2400-7. doi:10.2741/2853

9. Murphy PM. Neutrophil receptors for interleukin-8 and related CXC chemokines. *Semin Hematol*. Oct 1997;34(4):311-8.

10. Juss JK, House D, Amour A, et al. Acute Respiratory Distress Syndrome Neutrophils Have a Distinct Phenotype and Are Resistant to Phosphoinositide 3-Kinase Inhibition. *Am J Respir Crit Care Med*. Oct 15 2016;194(8):961-973. doi:10.1164/rccm.201509-1818OC

11. Ha H, Debnath B, Neamati N. Role of the CXCL8-CXCR1/2 Axis in Cancer and Inflammatory Diseases. *Theranostics*. 2017;7(6):1543-1588. doi:10.7150/thno.15625

12. Hosoki K, Itazawa T, Boldogh I, Sur S. Neutrophil recruitment by allergens contribute to allergic sensitization and allergic inflammation. *Curr Opin Allergy Clin Immunol*. Feb 2016;16(1):45-50. doi:10.1097/ACI.0000000000000231

13. Liu YW, Li S, Dai SS. Neutrophils in traumatic brain injury (TBI): friend or foe? *J Neuroinflammation*. May 17 2018;15(1):146. doi:10.1186/s12974-018-1173-x

14. Monin L, Khader SA. Chemokines in tuberculosis: the good, the bad and the ugly. *Semin Immunol*. Dec 2014;26(6):552-8. doi:10.1016/j.smim.2014.09.004

15. Khanam A, Trehanpati N, Riese P, Rastogi A, Guzman CA, Sarin SK. Blockade of Neutrophil's Chemokine Receptors CXCR1/2 Abrogate Liver Damage in Acute-

673 on-Chronic Liver Failure. *Front Immunol*. 2017;8:464.
674 doi:10.3389/fimmu.2017.00464
675 16. Grommes J, Soehnlein O. Contribution of neutrophils to acute lung injury. *Mol*
676 *Med*. Mar-Apr 2011;17(3-4):293-307. doi:10.2119/molmed.2010.00138
677 17. Russo RC, Garcia CC, Teixeira MM, Amaral FA. The CXCL8/IL-8 chemokine
678 family and its receptors in inflammatory diseases. *Expert Rev Clin Immunol*. May
679 2014;10(5):593-619. doi:10.1586/1744666X.2014.894886
680 18. Yin C, Liu B, Dong Z, et al. CXCL5 activates CXCR2 in nociceptive sensory
681 neurons to drive joint pain and inflammation in experimental gouty arthritis. *Nat*
682 *Commun*. Apr 16 2024;15(1):3263. doi:10.1038/s41467-024-47640-7
683 19. Santos I, Colaco HG, Neves-Costa A, et al. CXCL5-mediated recruitment of
684 neutrophils into the peritoneal cavity of Gdf15-deficient mice protects against
685 abdominal sepsis. *Proc Natl Acad Sci U S A*. Jun 2 2020;117(22):12281-12287.
686 doi:10.1073/pnas.1918508117
687 20. Wei L, Surma M, Shi S, Lambert-Cheatham N, Shi J. Novel Insights into the Roles
688 of Rho Kinase in Cancer. *Arch Immunol Ther Exp (Warsz)*. Aug 2016;64(4):259-
689 78. doi:10.1007/s00005-015-0382-6
690 21. Pernis AB, Ricker E, Weng CH, Rozo C, Yi W. Rho Kinases in Autoimmune
691 Diseases. *Annu Rev Med*. 2016;67:355-74. doi:10.1146/annurev-med-051914-
692 022120

693 22. Zhou Q, Gensch C, Liao JK. Rho-associated coiled-coil-forming kinases (ROCKs):
694 potential targets for the treatment of atherosclerosis and vascular disease. *Trends*
695 *Pharmacol Sci*. Mar 2011;32(3):167-73. doi:10.1016/j.tips.2010.12.006
696 23. Chen H, Hu X, Li R, et al. LncRNA THRIL aggravates sepsis-induced acute lung
697 injury by regulating miR-424/ROCK2 axis. *Mol Immunol*. Oct 2020;126:111-119.
698 doi:10.1016/j.molimm.2020.07.021
699 24. Xu H, Hou Q, Zhu J, Feng M, Wang P, Pan Y. The protective effect of Escherichia
700 coli Nissle 1917 on the intestinal barrier is mediated by inhibition of
701 RhoA/ROCK2/MLC signaling via TLR-4. *Life Sci*. Mar 1 2022;292:120330.
702 doi:10.1016/j.lfs.2022.120330
703 25. Chen R, Xu H, Guo Z, Zhang P, Chen J, Chen Z. CID16020046, a GPR55
704 antagonist, attenuates sepsis-induced acute kidney injury. *Mol Med Rep*. May
705 2022;25(5)doi:10.3892/mmr.2022.12671
706 26. Wang W, Wang LY, Zhao YY. Ginsenoside Rc Targets ROCK2 to Inhibit NF-
707 kappaB Activation and Alleviate Cognitive Dysfunction in Septic Encephalopathy
708 in vitro and in vivo. *Appl Biochem Biotechnol*. Nov 2025;197(11):7363-7376.
709 doi:10.1007/s12010-025-05372-4
710 27. Qian X, Yang L. ROCK2 knockdown alleviates LPS-induced inflammatory injury
711 and apoptosis of renal tubular epithelial cells via the NF-kappaB/NLRP3 signaling
712 pathway. *Exp Ther Med*. Sep 2022;24(3):603. doi:10.3892/etm.2022.11540

28. Yao J, Cheng M, Yang F. Calycosin Attenuates Lipopolysaccharide-Induced Acute Lung Injury in Mice through the miR-375-3p/ROCK2 Axis. *J Invest Surg*. Dec 2023;36(1):2211166. doi:10.1080/08941939.2023.2211166

29. Zhang X, Chen T, Li Z, et al. NORAD exacerbates metabolic dysfunction-associated steatotic liver disease development via the miR-511-3p/Rock2 axis and inhibits ubiquitin-mediated degradation of ROCK2. *Metabolism*. Mar 2025;164:156111. doi:10.1016/j.metabol.2024.156111

30. Zanin-Zhorov A, Chen W, Moretti J, et al. Selectivity matters: selective ROCK2 inhibitor ameliorates established liver fibrosis via targeting inflammation, fibrosis, and metabolism. *Commun Biol*. Nov 18 2023;6(1):1176. doi:10.1038/s42003-023-05552-0

31. Rittirsch D, Huber-Lang MS, Flierl MA, Ward PA. Immunodesign of experimental sepsis by cecal ligation and puncture. *Nat Protoc*. 2009;4(1):31-6. doi:10.1038/nprot.2008.214

32. Yin Z, Murphy MC, Li J, et al. Prediction of nonalcoholic fatty liver disease (NAFLD) activity score (NAS) with multiparametric hepatic magnetic resonance imaging and elastography. *Eur Radiol*. Nov 2019;29(11):5823-5831. doi:10.1007/s00330-019-06076-0

33. Wei J, Huang K, Chen Z, et al. Characterization of Glycolysis-Associated Molecules in the Tumor Microenvironment Revealed by Pan-Cancer Tissues and

733 Lung Cancer Single Cell Data. *Cancers (Basel)*. Jul 4
734 2020;12(7)doi:10.3390/cancers12071788
735 34. Zhu J, Huang Q, Liu S, et al. Construction of a Novel LncRNA Signature Related
736 to Genomic Instability to Predict the Prognosis and Immune Activity of Patients
737 With Hepatocellular Carcinoma. *Front Immunol*. 2022;13:856186.
738 doi:10.3389/fimmu.2022.856186
739 35. Yan J, Lei J, Chen L, et al. Human Leukocyte Antigen F Locus Adjacent Transcript
740 10 Overexpression Disturbs WISP1 Protein and mRNA Expression to Promote
741 Hepatocellular Carcinoma Progression. *Hepatology*. Dec 2018;68(6):2268-2284.
742 doi:10.1002/hep.30105
743 36. Landt SG, Marinov GK, Kundaje A, et al. ChIP-seq guidelines and practices of
744 the ENCODE and modENCODE consortia. *Genome Res*. Sep 2012;22(9):1813-
745 31. doi:10.1101/gr.136184.111
746 37. Zhang L, Liu Z, Li X, et al. Low long non-coding RNA HOTAIR expression is
747 associated with down-regulation of Nrf2 in the spermatozoa of patients with
748 asthenozoospermia or oligoasthenozoospermia. *Int J Clin Exp Pathol*.
749 2015;8(11):14198-205.
750 38. Bashir A, Wang M, Liu M, et al. Bach transcription factors: Emerging molecular
751 regulators for oxidative stress-mediated skin responses and protection. *J*
752 *Photochem Photobiol B*. Aug 2026;281:113491.
753 doi:10.1016/j.jphotobiol.2026.113491

754 39. Pradhan P, Vijayan V, Gueler F, Immenschuh S. Interplay of Heme with
755 Macrophages in Homeostasis and Inflammation. *Int J Mol Sci*. Jan 23
756 2020;21(3)doi:10.3390/ijms21030740
757 40. Zhu J, Zhao J, Luo C, et al. FAT10 promotes chemotherapeutic resistance in
758 pancreatic cancer by inducing epithelial-mesenchymal transition via stabilization
759 of FOXM1 expression. *Cell Death Dis*. May 25 2022;13(5):497.
760 doi:10.1038/s41419-022-04960-0
761 41. Srdic T, Durasevic S, Lakic I, et al. From Molecular Mechanisms to Clinical
762 Therapy: Understanding Sepsis-Induced Multiple Organ Dysfunction. *Int J Mol*
763 *Sci*. Jul 16 2024;25(14)doi:10.3390/ijms25147770
764 42. Xu X, Yang T, An J, Li B, Dou Z. Liver injury in sepsis: manifestations,
765 mechanisms and emerging therapeutic strategies. *Front Immunol*.
766 2025;16:1575554. doi:10.3389/fimmu.2025.1575554
767 43. Lelubre C, Vincent JL. Mechanisms and treatment of organ failure in sepsis. *Nat*
768 *Rev Nephrol*. Jul 2018;14(7):417-427. doi:10.1038/s41581-018-0005-7
769 44. Nagai Y, Matoba K, Nishimura R. ROCK signaling at the crossroads of redox
770 stress, mitochondrial dynamics, and metabolic disease. *Redox Biol*. May
771 2026;92:104109. doi:10.1016/j.redox.2026.104109
772 45. Liu J, Wu YH, Zhang ZL, Li P. Tanshinone IIA improves sepsis-induced acute
773 lung injury through the ROCK2/NF-kappaB axis. *Toxicol Appl Pharmacol*. Jul 1
774 2022;446:116021. doi:10.1016/j.taap.2022.116021

46. Jianjun Z, Baochun Z, Limei M, Lijun L. Exploring the beneficial role of ROCK inhibitors in sepsis-induced cerebral and cognitive injury in rats. *Fundam Clin Pharmacol*. Oct 2021;35(5):882-891. doi:10.1111/fcp.12645

47. Hu Y, Yang B, Xiao C, et al. Selective targeting of endothelial and perivascular angiocrine ROCK2 treats liver fibrosis. *Cell*. Apr 30 2026;189(9):2663-2683 e26. doi:10.1016/j.cell.2026.02.001

48. Liu C, Cai Y, Mou S. Exploring the mechanism of polymorphonuclear neutrophils against sepsis based on immune model. *Ann Med*. Dec 2026;58(1):2640268. doi:10.1080/07853890.2026.2640268

49. Rajarathnam K, Schnoor M, Richardson RM, Rajagopal S. How do chemokines navigate neutrophils to the target site: Dissecting the structural mechanisms and signaling pathways. *Cell Signal*. Feb 2019;54:69-80. doi:10.1016/j.cellsig.2018.11.004

50. Bu Y, Li Z, Wang C, et al. The MafG/Bach1-Lcn2 transcriptional axis drives ferroptosis in sepsis-induced acute lung injury via disrupting redox homeostasis. *Free Radic Biol Med*. Mar 1 2026;245:250-268. doi:10.1016/j.freeradbiomed.2025.12.050

51. Cai L, Arbab AS, Lee TJ, et al. BACH1-Hemoxygenase-1 axis regulates cellular energetics and survival following sepsis. *Free Radic Biol Med*. Aug 1 2022;188:134-145. doi:10.1016/j.freeradbiomed.2022.06.005

795 52. Liu T, Yu X, Li G, et al. Rock2 regulates Cdc25A through ubiquitin proteasome
796 system in hepatocellular carcinoma cells. *Exp Cell Res*. Oct 1 2012;318(16):1994-
797 2003. doi:10.1016/j.yexcr.2012.04.017
798 53. Huang D, Du X, Yuan R, et al. Rock2 promotes the invasion and metastasis of
799 hepatocellular carcinoma by modifying MMP2 ubiquitination and degradation.
800 *Biochem Biophys Res Commun*. Oct 10 2014;453(1):49-56.
801 doi:10.1016/j.bbrc.2014.09.061
802 54. Deng X, Yi X, Deng J, et al. ROCK2 promotes osteosarcoma growth and
803 metastasis by modifying PFKFB3 ubiquitination and degradation. *Exp Cell Res*.
804 Dec 15 2019;385(2):111689. doi:10.1016/j.yexcr.2019.111689
805 55. Abdelrheem NM, Ahmed MAE, Mohamed AF, El Sayed NS, Shalaby HN. Anti-
806 inflammatory and antinociceptive effects of fasudil in a reserpine-induced
807 fibromyalgia model: Role of ROCK-regulated leptin-STAT3 signaling. *Life Sci*.
808 Jun 15 2026;395:124372. doi:10.1016/j.lfs.2026.124372
809 56. Muraoka S, Izumi T, Nishida K, et al. RECOVER study: a multicenter
810 retrospective cohort study and comparison of the efficacy and safety of
811 clazosentan and fasudil in patients with aneurysmal subarachnoid hemorrhage. *J*
812 *Neurosurg*. Sep 1 2025;143(3):624-633. doi:10.3171/2025.1.JNS242509
813 57. Braegelmann C, Niebel D, Ferring-Schmitt S, et al. Epigallocatechin-3-gallate
814 exhibits anti-inflammatory effects in a human interface dermatitis model-

implications for therapy. *J Eur Acad Dermatol Venereol*. Jan 2022;36(1):144-153. doi:10.1111/jdv.17710

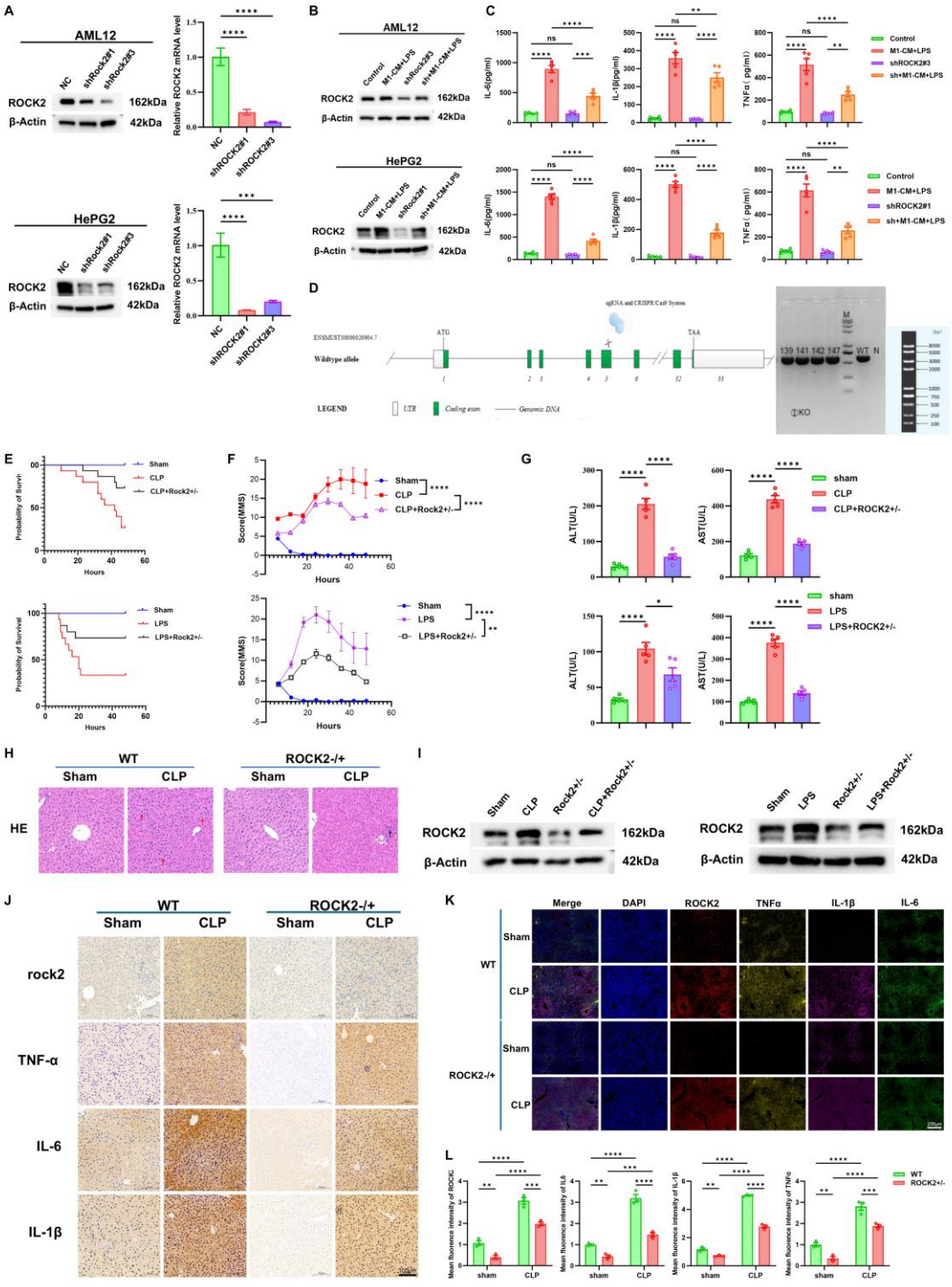
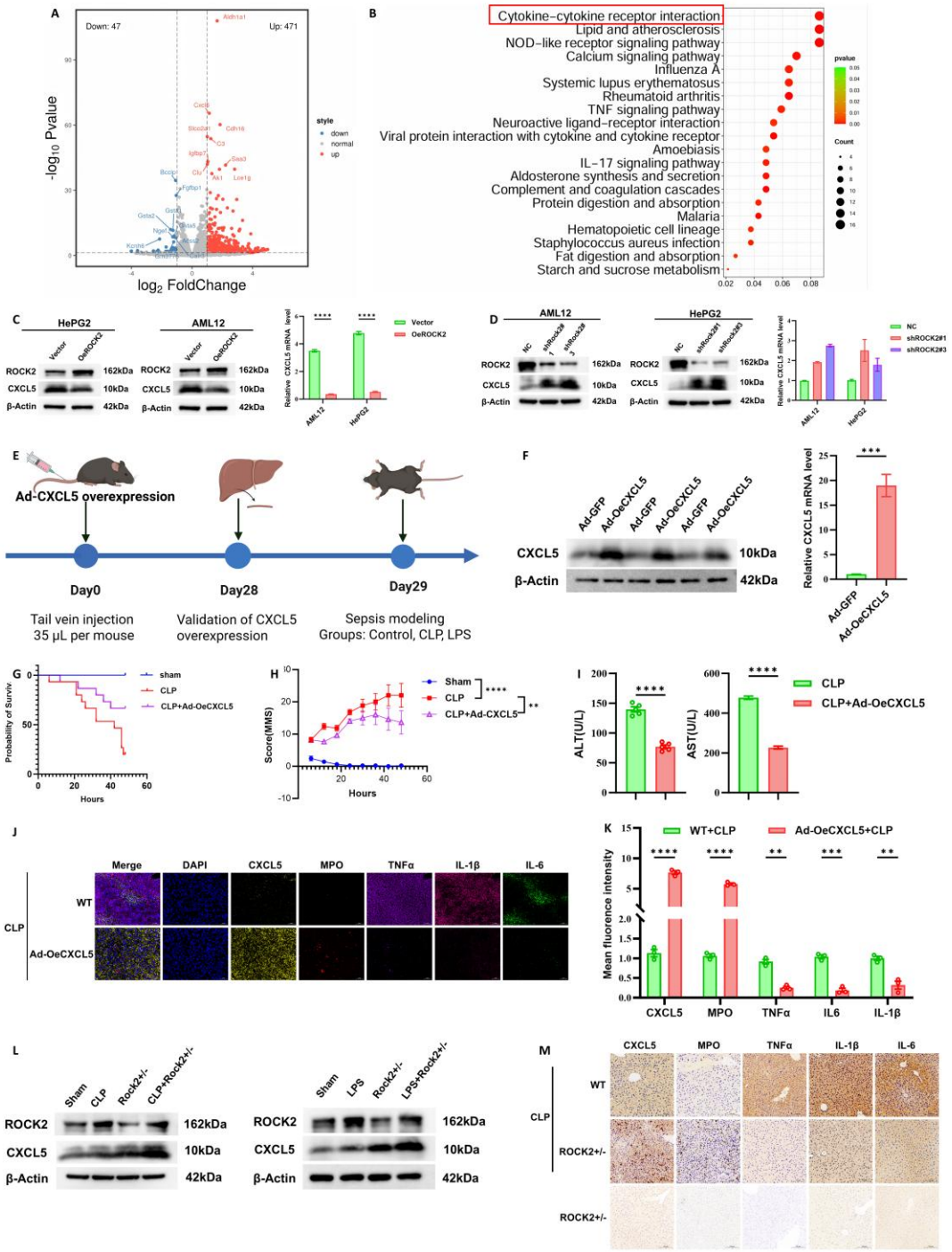


Fig. 2 ROCK2 downregulation alleviates sepsis-associated liver injury.

A Western blotting and quantitative real-time PCR (qRT–PCR) validation of ROCK2 knockdown in AML12 and HepG2 cells; B Western blotting analysis of ROCK2 in M1-CM/LPS-treated cells with or without ROCK2 knockdown; C ELISA

of IL-6, IL-1β and TNFα in the indicated cell groups; D CRISPR/Cas9 targeting strategy and genotyping of Rock2 heterozygous mice; E Kaplan–Meier survival curves after CLP or LPS challenge; F MMS over time; G Serum ALT and AST levels; H Representative H&E staining of liver sections; I Western blotting analysis of hepatic ROCK2; J Representative immunohistochemical staining of ROCK2, TNFα, IL-6 and IL-1β (scale bar, 100 μm); K Representative immunofluorescence staining of ROCK2, TNFα, IL-1β and IL-6 (scale bar, 200 μm); L Quantification of mean fluorescence intensity in K. *$p < 0.05$; **$p < 0.01$; ***$p < 0.001$; ****$p < 0.0001$; ns, not significant.



850

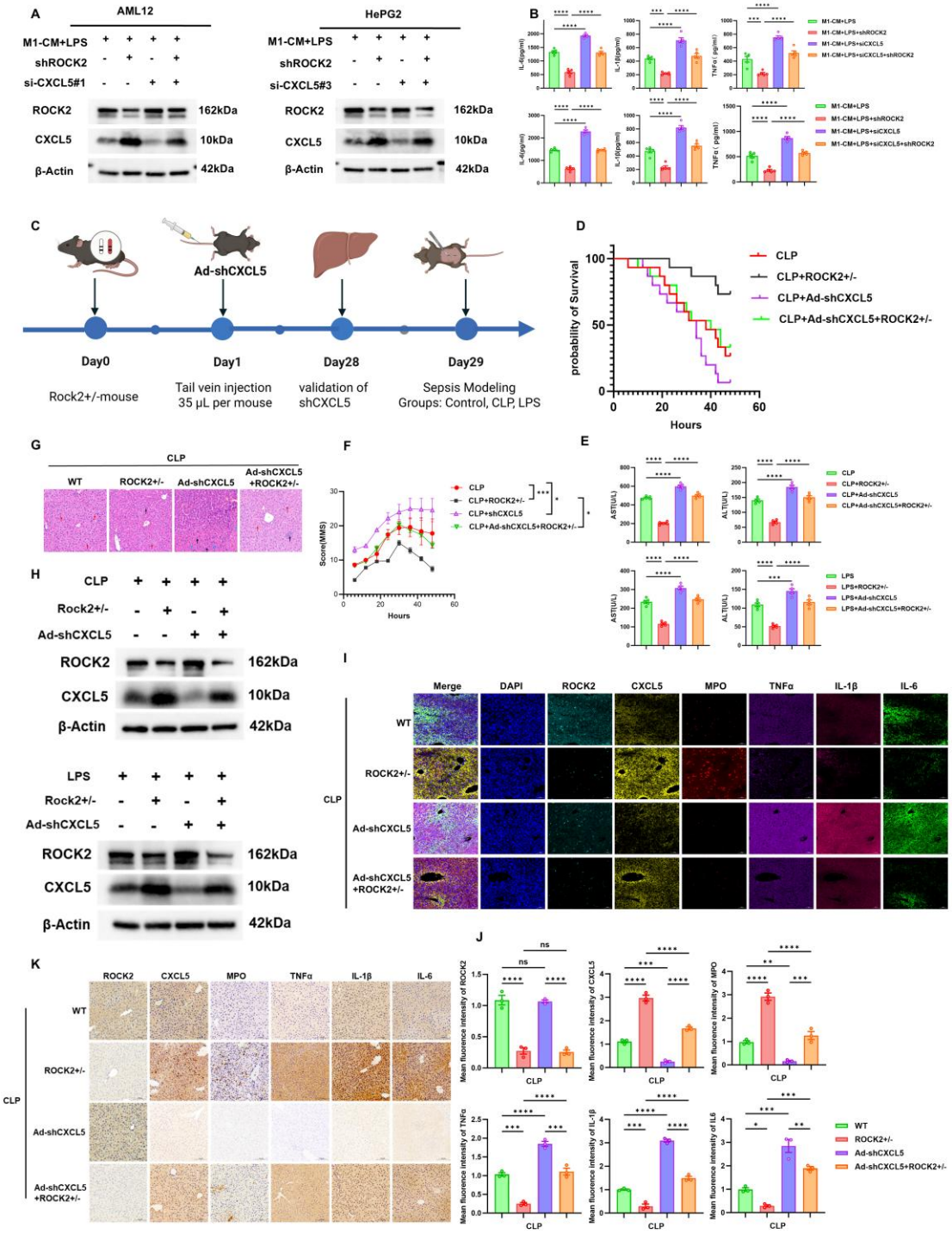
851 **Fig. 3 ROCK2 deficiency promotes CXCL5 expression and neutrophil recruitment**

852 **during sepsis-associated liver injury.**

853 A Volcano plot of differentially expressed genes between M1-CM/LPS-treated

854 control and ROCK2-knockdown AML12 cells; B KEGG pathway enrichment analysis;

C Western blotting analysis of ROCK2 and CXCL5 and qRT–PCR analysis of CXCL5 in ROCK2-overexpressing HepG2 and AML12 cells; D Western blotting analysis of ROCK2 and CXCL5 and qRT–PCR analysis of CXCL5 in ROCK2-knockdown AML12 and HepG2 cells; E Experimental schedule for hepatic CXCL5 overexpression and CLP/LPS modelling; F Western blotting and qRT–PCR validation of hepatic CXCL5 overexpression; G Kaplan–Meier survival curves after CLP; H MMS over time; I Serum ALT and AST levels; J Representative immunofluorescence staining of CXCL5, myeloperoxidase (MPO), TNFα, IL-1β and IL-6 in liver sections; K Quantification of mean fluorescence intensity in J; L Western blotting analysis of hepatic ROCK2 and CXCL5 in CLP- and LPS-challenged wild-type and Rock2 heterozygous mice; M Representative immunohistochemical staining of CXCL5, MPO, TNFα, IL-1β and IL-6 in liver sections. Scale bars are as indicated. *$p < 0.05$; **$p < 0.01$; ***$p < 0.001$; ****$p < 0.0001$; ns, not significant.



869

870 **Fig. 4 CXCL5 silencing reverses the protective effects of ROCK2 deficiency in**

871 **sepsis-associated liver injury.**

872 A Western blotting analysis of ROCK2 and CXCL5 in M1-CM/LPS-treated

873 AML12 and HepG2 cells after ROCK2 and/or CXCL5 silencing; B ELISA of IL-6, IL-

1β and TNFα in the indicated cell groups; C Experimental schedule for hepatic CXCL5 silencing in Rock2 heterozygous mice and CLP/LPS modelling; D Kaplan–Meier survival curves after CLP; E Serum ALT and AST levels after CLP or LPS challenge; F MMS over time; G Representative H&E staining of liver sections; H Western blotting analysis of hepatic ROCK2 and CXCL5 after CLP or LPS challenge; I Representative immunofluorescence staining of ROCK2, CXCL5, MPO, TNFα, IL-1β and IL-6 in liver sections; J Quantification of mean fluorescence intensity in I; K Representative immunohistochemical staining of ROCK2, CXCL5, MPO, TNFα, IL-1β and IL-6 in liver sections. Scale bars are as indicated. *$p < 0.05$; **$p < 0.01$; ***$p < 0.001$; ****$p < 0.0001$; ns, not significant.

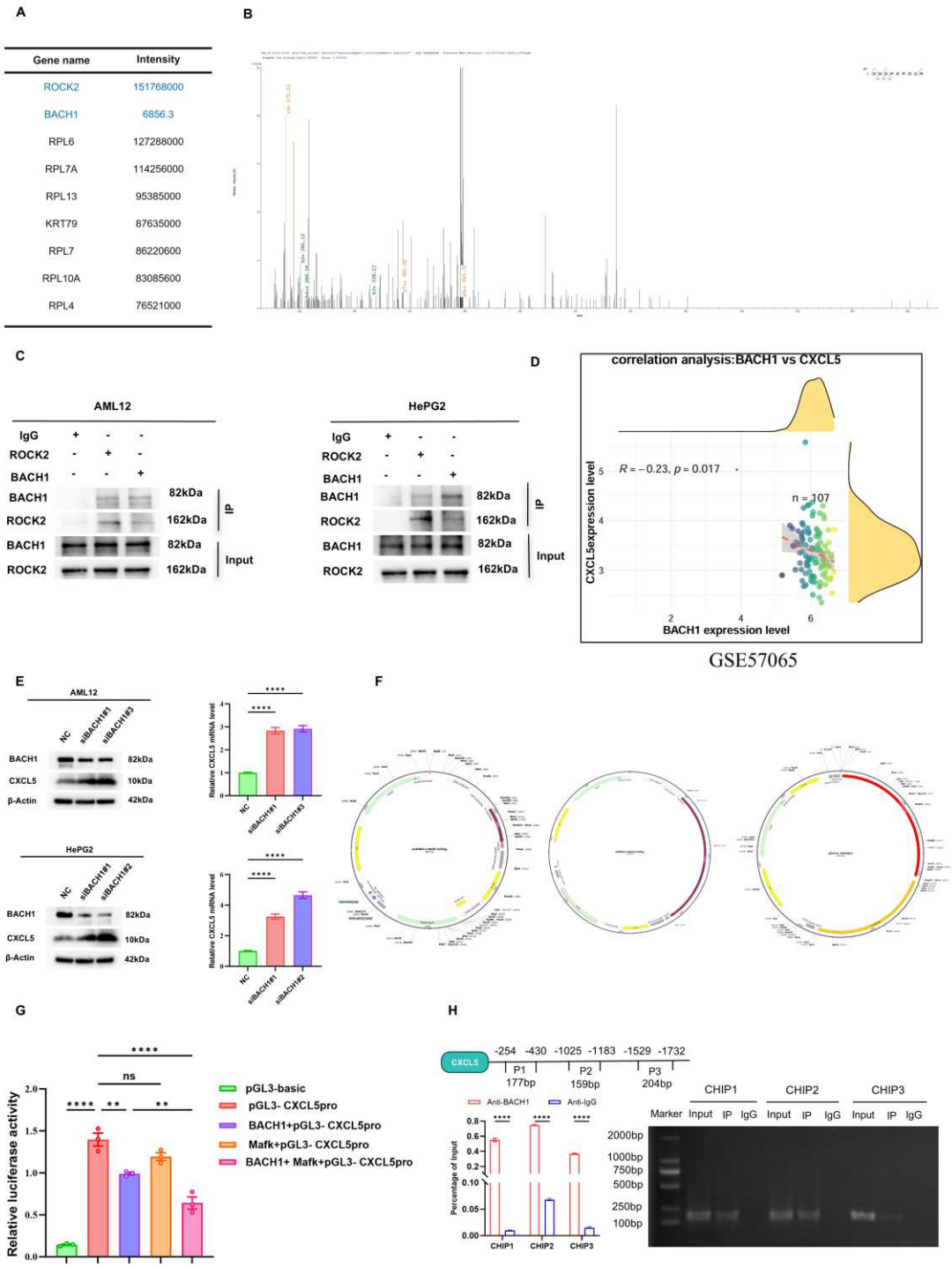


Fig. 5 ROCK2 interacts with BACH1, which represses CXCL5 transcription.

A Candidate ROCK2-interacting proteins identified by co-immunoprecipitation coupled with mass spectrometry (Co-IP–MS); B Tandem mass spectrum of a BACH1-derived peptide; C Reciprocal endogenous Co-IP analysis of ROCK2 and BACH1 in

AML12 and HepG2 cells; D Correlation analysis of BACH1 and CXCL5 expression in the GSE57065 dataset; E Western blotting analysis of BACH1 and CXCL5 and qRT–PCR analysis of CXCL5 after BACH1 silencing in AML12 and HepG2 cells; F Maps of the MAFK and BACH1 expression vectors and the CXCL5 promoter reporter construct; G Dual-luciferase reporter analysis of CXCL5 promoter activity in the indicated transfection groups; H Schematic of the CXCL5 promoter regions analysed by chromatin immunoprecipitation (ChIP), ChIP–qPCR analysis and representative agarose gel electrophoresis. **$p < 0.01$; ****$p < 0.0001$; ns, not significant.

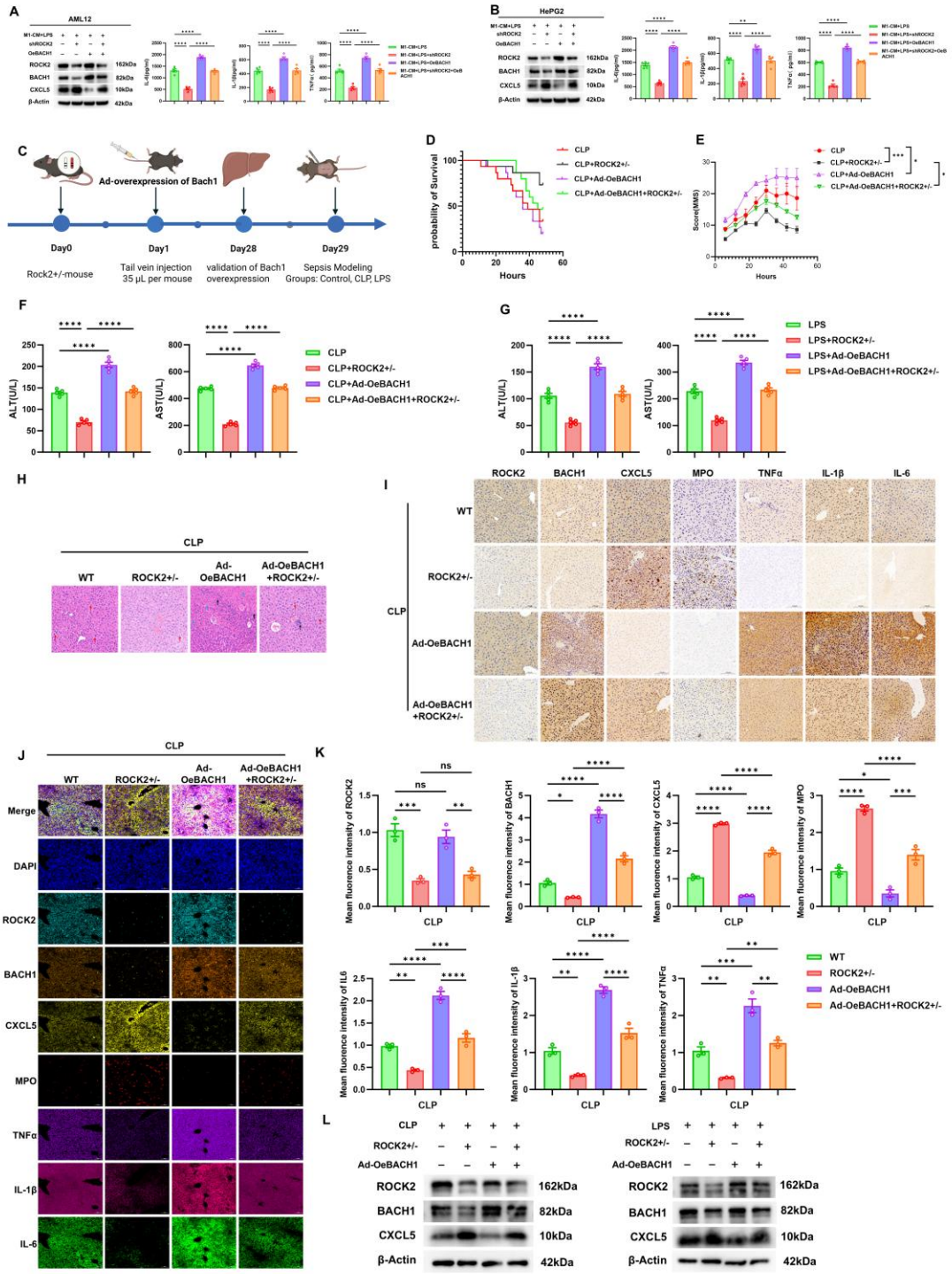


Fig. 6 BACH1 overexpression reverses the protective effects of ROCK2 deficiency in sepsis-associated liver injury.

A, B Western blotting analysis of ROCK2, BACH1 and CXCL5 and ELISA of IL-6, IL-1β and TNFα in M1-CM/LPS-treated AML12 and HepG2 cells after ROCK2

knockdown and/or BACH1 overexpression; C Experimental schedule for hepatic BACH1 overexpression in Rock2 heterozygous mice and CLP/LPS modelling; D Kaplan–Meier survival curves after CLP; E MMS over time; F Serum ALT and AST levels after CLP; G Serum ALT and AST levels after LPS challenge; H Representative H&E staining of liver sections; I Representative immunohistochemical staining of ROCK2, BACH1, CXCL5, MPO, TNFα, IL-1β and IL-6 in liver sections; J Representative immunofluorescence staining of ROCK2, BACH1, CXCL5, MPO, TNFα, IL-1β and IL-6 in liver sections; K Quantification of mean fluorescence intensity in J; L Western blotting analysis of hepatic ROCK2, BACH1 and CXCL5 after CLP or LPS challenge. Scale bars are as indicated. *$p < 0.05$; **$p < 0.01$; ***$p < 0.001$; ****$p < 0.0001$; ns, not significant.

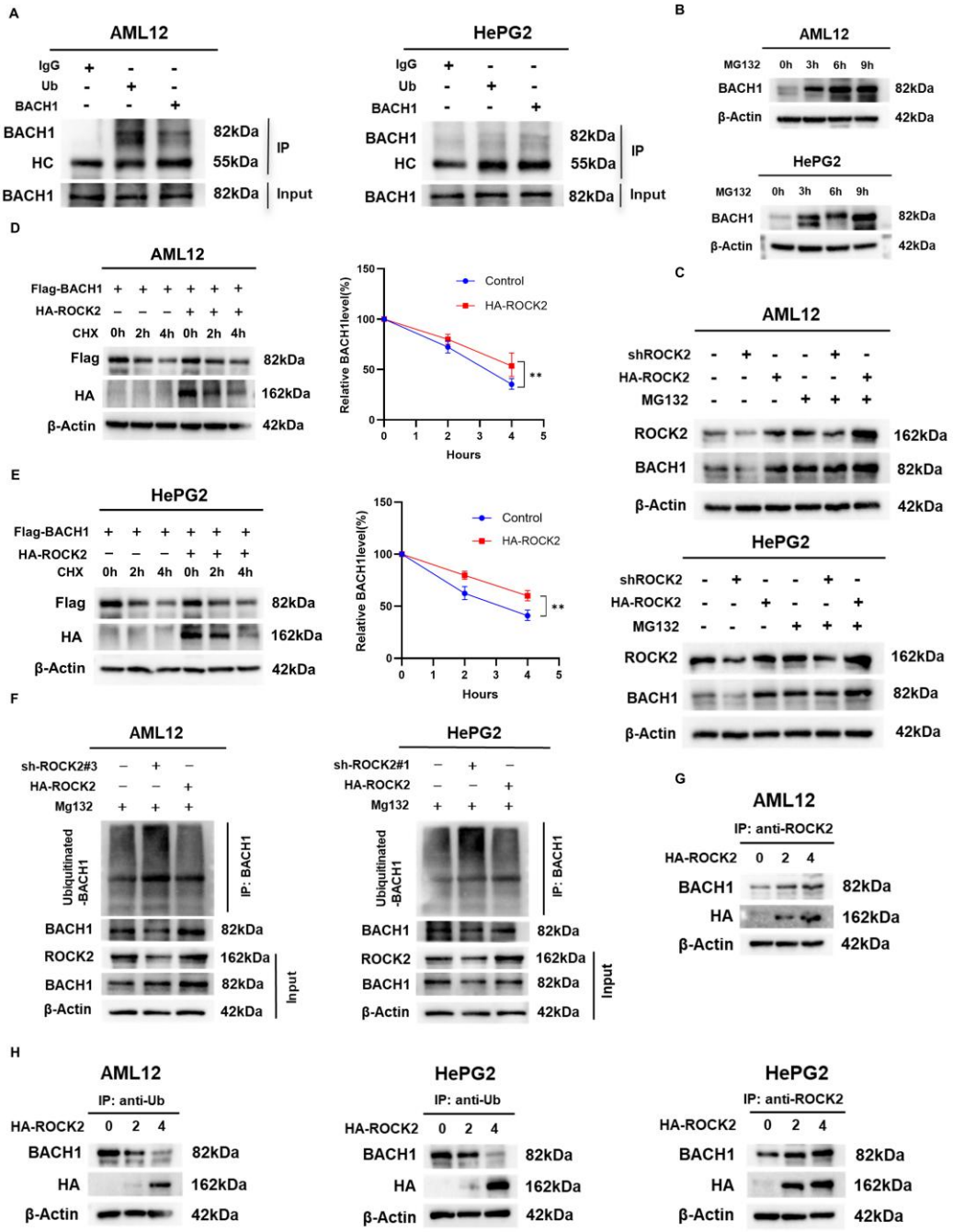


Fig. 7 ROCK2 stabilises BACH1 by limiting its ubiquitin-mediated proteasomal degradation.

A Co-IP analysis of BACH1 and ubiquitin in AML12 and HepG2 cells; B Western blotting analysis of BACH1 after treatment with the proteasome inhibitor MG132 for

921 the indicated times; C Western blotting analysis of ROCK2 and BACH1 after ROCK2
922 knockdown or overexpression with or without MG132; D, E Cycloheximide (CHX)-
923 chase analysis and quantification of BACH1 protein stability in AML12 and HepG2
924 cells with or without ROCK2 overexpression; F Immunoprecipitation analysis of
925 BACH1 ubiquitination after ROCK2 knockdown or overexpression in AML12 and
926 HepG2 cells; G, H Dose-dependent immunoprecipitation analyses of ROCK2–BACH1
927 association and BACH1 ubiquitination in AML12 and HepG2 cells. **$p < 0.01$.
928

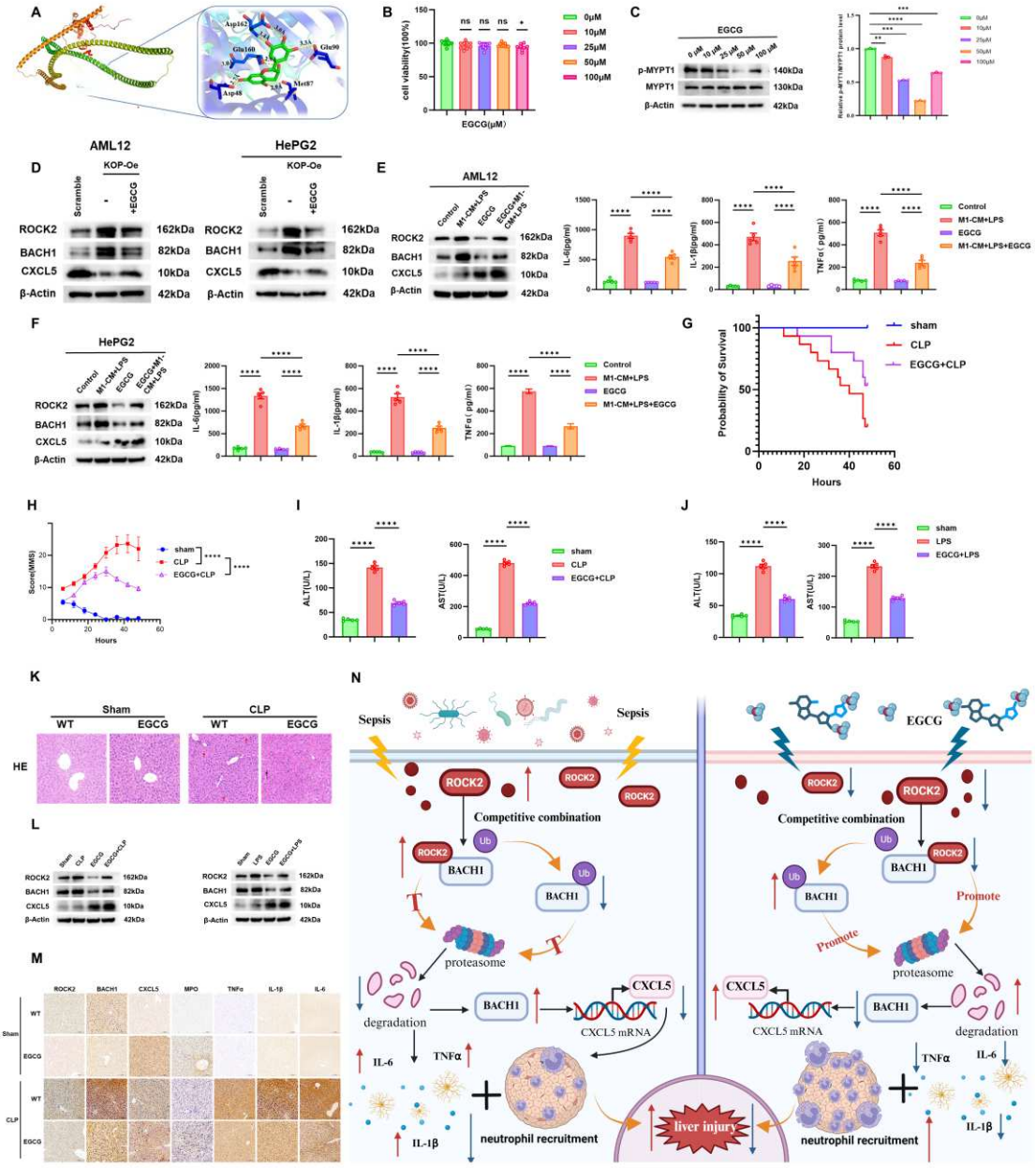


Fig. 8 Epigallocatechin gallate targets ROCK2 and alleviates sepsis-associated liver injury.

A Molecular docking model of epigallocatechin gallate (EGCG) binding to ROCK2; B CCK-8 analysis of cell viability after treatment with the indicated EGCG

concentrations; C Western blotting and densitometric analyses of phosphorylated MYPT1 and total MYPT1 after EGCG treatment; D Western blotting analysis of ROCK2, BACH1 and CXCL5 in ROCK2-overexpressing AML12 and HepG2 cells with or without EGCG; E, F Western blotting analysis of ROCK2, BACH1 and CXCL5 and ELISA of IL-6, IL-1β and TNFα in M1-CM/LPS-treated AML12 and HepG2 cells with or without EGCG; G Kaplan–Meier survival curves after CLP; H MMS over time; I Serum ALT and AST levels after CLP; J Serum ALT and AST levels after LPS challenge; K Representative H&E staining of liver sections; L Western blotting analysis of hepatic ROCK2, BACH1 and CXCL5 after CLP or LPS challenge; M Representative immunohistochemical staining of ROCK2, BACH1, CXCL5, MPO, TNFα, IL-1β and IL-6 in liver sections; N Working model summarising the ROCK2–BACH1–CXCL5 axis and EGCG intervention in sepsis-associated liver injury. Scale bars are as indicated. *$p < 0.05$; **$p < 0.01$; ***$p < 0.001$; ****$p < 0.0001$; ns, not significant.

Supplementary Files

This is a list of supplementary files associated with this preprint. Click to download.

- TableS1Primersequences.xlsx
- figureS1.pdf